INDONESIAN JOURNAL ON GEOSCIENCE
Geological Agency
Ministry of Energy and Mineral Resources

Journal homepage: http://ijog.geologi.esdm.go.id
ISSN 2355-9314, e-ISSN 2355-9306

Characterization of Carbonate Reservoir Potential in Salawati Basin, West Papua: Analysis of Seismic Direct Hydrocarbon Indicator (DHI), Seismic Attributes, and Seismic Spectrum Decomposition

Handoyo Handoyo[1], Bernard Cavin Ronlei[1], Asido Saputra Sigalingging[1], Per Avseth[2], Endra Triyana[3], Özgenç Akin[4], Paul Young[5], Juan Alcalde[6] and Ramon Carbonell[6]

[1]Teknik Geofisika Institut Teknologi Sumatera, South Lampung, Indonesia
[2]Dig Science, Oslo, Norway
[3]SKK MIGAS, Jl. Gatot Subroto, Jakarta, Indonesia
[4]Department of Geophysical Engineering, Karadeniz Technical University, Trabzon, Turkey
[5]TGS NOPEC Geophysical Company ASA, Perth, Australia
[6]Geosciences Barcelona (GEO3BCN, CSIC), 08028 Barcelona, Spain

Corresponding author: handoyo.geoph@tg.itera.ac.id
Manuscript received: September, 27, 2023; revised: April, 28, 2024;
approved: May, 4, 2024; available online: July, 2, 2024

Abstract - Carbonate reservoir of Kais Formation in Salawati Basin, West Papua, is the most famous oil and gas reservoir in the eastern part of Indonesian Archipelago since 1970's. Nowadays, new prospects in this area are more challenging and most relevant near the infrastructure of previous oil and gas fields. In this study, a relatively new seismic dataset was investigated to figure out new prospects in carbonate reservoir rocks in the area of interest. In this preliminary study, where seismic data are not supported by well data, direct hydrocarbon indicator (DHI), seismic attribute, and spectral decomposition (CWT: continuous wavelet transform) allow the authors to characterize the reservoir geometry and to predict pore fluids within the reservoir rocks. The reservoir geometry of carbonate reef of Kais Formation (C1) was identified by seismic reflectors with high amplitude contrast at the top C1. The hydrocarbon indicator was predicted by DHI where dim spots, flat spots, and polarity reversals are indicative of hydrocarbon prospects. From the attribute analysis, the attribute instantaneous amplitude detected the top carbonate C1, whereas pore fluids were predicted from high sweetness attribute. In addition, spectral decomposition CWT method confirms the top C1, identified as saturated rock by the frequency of 10 Hz, 20 Hz, and 30 Hz. Based on a seismic study in the researched area, the target zone is expected to be a very promising hydrocarbon reservoir, specifically a carbonate reservoir. As a result, the preferred well-test location is in a region with access to the Kais Formation limestone reef layer. This study can assist in reservoir characterization, especially in areas with limited well control.

Keywords: carbonate reservoir, DHI, CWT, frequency, seismic attribute, spectral decomposition

How to cite this article:
Handoyo, H., Ronlei, B.C., Sigalingging, A.S., Avseth, P., Triyana, E., Akin, Ö., Young, P., Alcalde, J., and Carbonell, R., 2024. Characterization of Carbonate Reservoir Potential in Salawati Basin, West Papua: Analysis of Seismic Direct Hydrocarbon Indicator (DHI), Seismic Attributes, and Seismic Spectrum Decomposition. *Indonesian Journal on Geoscience*, 11 (2), p.173-188. DOI: 10.17014/ijog.11.2.173-188

Introduction

Background

For the purpose to identify new feasible areas or to enhance production, efforts to comprehend the properties of reservoir rocks have always been conducted and will continue to be performed both at existing locations and at new places. One of the reservoirs in Indonesia with the potential to produce hydrocarbons is the carbonate reservoir,

particularly in the east of the country. West Papua is one of the regions that has experienced development in exploration and exploitation studies (geological setting, basin history, and stratigraphy) since the 1970s (Redmond and Koesoemadinata, 1976; Phoa and Samuel, 1986; Robinson, 1987; Satyana, 2003). To locate new areas of potential for carbonate reservoirs, researchers are still investigating the Salawati Basin area. Therefore, this study addresses methods to comprehend carbonate reservoir rock features using seismic data in the absence of well data. An overview of the prospect zone in the Salawati Basin, West Papua, is provided in this research as the first step or preliminary investigation.

The seismic method allows the authors to perform seismic characterization of the reservoir rock (Palaz and Marfurt, 1997; Liu and Wang, 2017; Handoyo *et al*., 2020; Teillet *et al*., 2021; Avseth and Lehocki, 2021). Several techniques include direct hydrocarbon indicator (DHI), attribute seismic, and spectral decomposition. Several workers (Cooke, 1993; Li *et al*., 2011; Nanda, 2021) have reported that one or a combination of these methods can be used for initial studies of the potential of a reservoir rock, both in clastic and carbonate sediments. The DHI method utilizes impedance contrast, which is represented by amplitude, seismic phase, and also the typical shape (geometry) of carbonate rocks such as buildup or reef (Castagna *et al*., 1995; Shadlow, 2014). Seismic DHI characteristics of gas accumulations, such as gas chimneys, dim spots, and flat spots, as well as associated events, such as a decrease in velocity (time sag), downward pressure, frequency reduction, and polarity reversals discovered in seismic profiles, are additionally applicable as indicators. The seismic attribute methods such as instantaneous amplitude, frequency, and sweetness can be applied to characterize lithological changes from seismic energy responses and fluids from frequency and sweetness responses (Vincentelli *et al*., 2014; Rosa *et al.*, 2017; Do Nascimento *et al.*, 2017). In addition, the spectral decomposition (CWT) method can be used to predict the presence of fluid by varying the frequency and energy spectrum values in the target zone (Yu *et al*., 2013; Li *et al*., 2016; Naseer and Asim, 2018). Moreover, the results of this research are expected to provide recommendations for the location of appraisal and production wells. Finally, it is intended that this research will be able to contribute to a preliminary framework to comprehend the properties of reservoir rocks, particularly in areas where there are limited well data.

Geological/Stratigraphical Settings

According to Dow and Sukamto (1984), Papua is divided into three main parts, namely the Bird Head, Bird Body, and Bird Tail (Figure 1). The Bird Head is located on the peninsula to the north, which is joined by the neck to the main body.While, the Bird Body is the mainland part of New Guinea (Papua) Island, and the Bird Tail is located in the eastern part of Papua New Guinea Island.

The Salawati Basin is in the Bird Head section. The landscapes found at the Bird Head include hills, intermountain valleys, karst hills and mountains, littoral plains, alluvial plains, and uplifted coral reefs.

Most of the Bird Head area is composed of continental crust which is part of northwestern Australia. The collision between the continental plate northwest of Australia and the Pacific Ocean Plate and the collision between the Banda Sea Ocean Plate in the southwest are signs of Neogene tectonics in Papua (Hamilton, 1979). The collision between the Pacific Ocean Plate and the Australian Plate formed a convergent strike-slip fault along the Papua area, and produced a strike-slip fault and a factoring fault along Papua. In line with their relative position in Neogene stress conditions, left-hand strike faults and factoring faults are activations of old faults trending N300^{o}E and west - east. The path of factoring and fold fault structures in the Lengguru Zone is formed from old north - south oriented structures such as the Lengguru Fold Belt (Sapiie and Cloos, 2004).

The Salawati Basin has a very intensive structure. The dominating structure is a normal fault which generally trends SW - NE and to the north or west which indicates a subsidence of the basin. The horizontal fault zone of Sorong Fault has a WSW to ENE directions forming the principal displacement

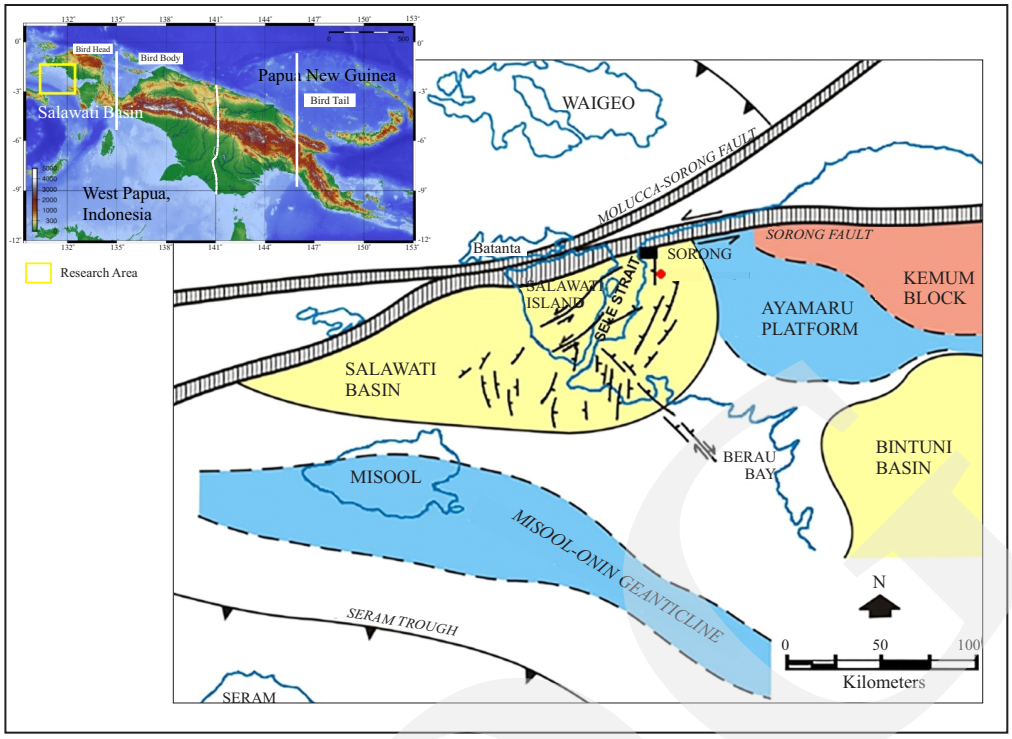

Figure 1. Location and geological setting of Salawati Basin, West Papua (modiefied from Satyana *et al.*, 2003).

zone and limiting the basin to the north. Synthetic left fault and Salawati Fault cross Salawati Island in a SW - NE direction that connected to the Sorong Fault. The Salawati Fault also shows a normal slip and has partially accommodated the subsidence of the basin towards the north. A horizontal fault to the right of Cendrawasih trending NW – SE extends from the south of the Sele Strait to the SE to the area near the Bintuni Basin. This fault is thought to be a Paleozoic or Mesozoic fault which is activated to become a dextral slip by the Sorong Fault (Satyana *et al.*, 2003).

In Figure 2 (Satyana *et al.*, 2003), the stratigraphy in Salawati Basin comprises several formations from the oldest to the youngest including Pretertiary basement, Imskin Formation (Paleocene - Late Middle Eocene), Faumai Formation (Late Eocene - Early Oligocene), Sirga Formation (Late Oligocene), Kais Formation (Early Miocene - Late Miocene), Klasafet Formation (Middle Miocene - Late Miocene), Klasaman Formation (Pliocene), and Sele Formation (Pleistocene). In this study, the focus of the study was on the Kais Formation (Early Miocene - Late Miocene), Klasafet Formation (Middle Miocene - Late Miocene), and Klasaman Formation (Pliocene).

In Figure 2, the Sirga Formation is overlain by the Kais Formation. It was deposited in Late Oligocene as siltstone, shelf limestone, and reef limestone above a transgressive unconformity. Based on seismicity, the Kais Formation is divided into the Lower Kais Formation and the Upper Kais Formation (Sudirja and Robinson, 1986; Pireno, 2017). The Lower Kais Formation or intra-Kais horizon which is Early Miocene in age is composed of shelf limestone and reef limestone. These rocks were deposited in a wide shallow marine environment and only developed in the Matoa Subbasin, located in the northern part of the Salawati Basin. In the deposition of the Lower Kais Formation, there was a brief drop in the sea level which resulted in the limestone of this formation being exposed to the surface and producing secondary porosity.

Then, the Klasafet Formation (Sudirja and Robinson, 1986; Pireno, 2017) deposited in the transgression phase in a closed, shallow marine environment, comprises mudstone or clay intercalated with thin limestone that slopes over the limestone of the Kais Formation (play the role of caprock of the

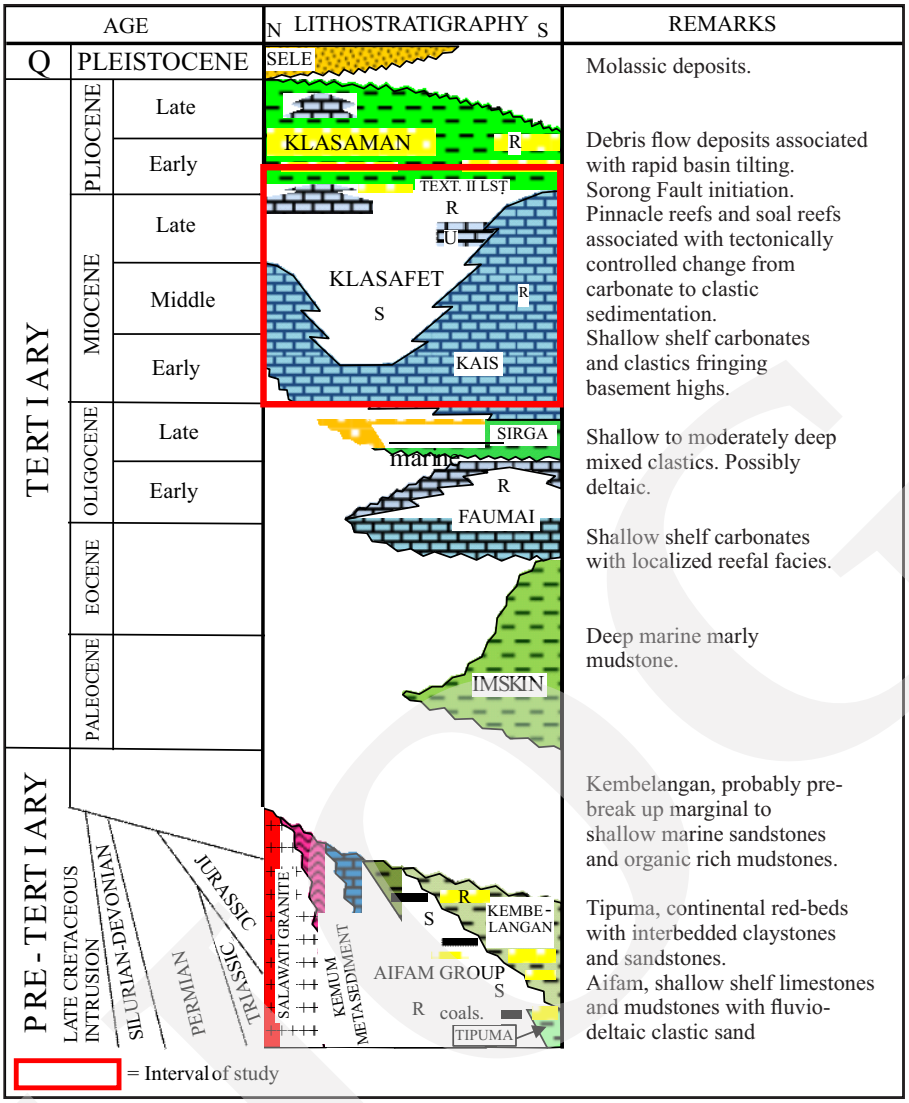

Figure 2. Regional stratigraphy of Salawati Basin, West Papua (modified from Sudirja and Robinson, 1986; Satyana *et al*., 2003; Pireno, 2017).

limestone reservoir of Kais Formation) in the north and south. The deposition of Klasafet Formation ended with the deposition of deep-sea limestone or textularia limestone and reef limestone in high areas in the northwestern part of the basin (Sudirja and Robinson, 1986; Pireno, 2017).

Additionally, Saputra et al. (2023) stated that Kemum Block, located in the northern Bird Head Peninsula of Papua Island, is an extension of Paleozoic to Early Mesozoic Pacific-facing active margin of East Gondwana, associated with Mid Paleozoic orogenic deformation and foreland basin deposition. The NNW trending fold affected the Mesozoic-Paleogene succession of the northern Lengguru Fold Belt leading to the presence of WSW mostly moderately-gently dips. Moreover, the Pliocene – Quaternary Central Bird Head Monocline was influenced by the structures in the northern Lengguru Fold Belt, associated with the uplifting of Kemum Block in the northern Bird Head Peninsula.

Methods and Materials

Methods

In this study, the method used to achieve the objectives includes: (i) seismic direct hydrocarbon indicator (DHI); (ii) seismic attributes; and (iii) seismic spectral decomposition.

Seismic Direct Hydrocarbon Indicator (DHI)

Seismic interpretation and analysis of the studied area revealed the presence of direct hydrocarbon indicators that can be used to forecast the presence of an accumulation of hydrocarbons in the reef limestone of Kais Formation C1. In this study, a symple theoretical/model of reservoir parameters was created in limestone model. In Figure 3, reef carbonate C1 has higher density and velocity than the clay of Kais Formation at the top of C1. This situation will create a DHI response of dim spot between clay and limestone with a high contrast positive reflection coefficient (Forrest *et al*., 2010; Zdanowski and Górniak, 2014; Howarth and Alves, 2016). Moreover, flat spots characterized by horizontal reflections are observed in the seismic data. These are thought to be strong indicators of the presence of gas in subsurface, where the horizontal events represent gas-water contacts (Chopra and Marfurt, 2012; Kluesner *et al*., 2013; Neidell and Charuk, 2018).

The presence of hydrocarbons in the reservoir causes the velocity to decrease, which potentially causes the polarity of the reflected wavelets to reverse (Nanda, 2021). This change in sign occurs at the top of the reservoir. Meanwhile, the polarity reversals have been attributed to abrupt differences in the physical characteristics of nearby lithofacies or by the presence of hydrocarbons (Barnes, 2001). In addition, one of the direct hydrocarbon indicators that indicates the presence of a massive gas reservoir in the interest zone is the gas chimney (cloud). Gas from the deeper reservoir leaks upward, creating the gas chimney. It has a cloudy appearance that resembles cigarette smoke zone (Arntsen *et al*., 2007; Petersen *et a*l., 2010; Dixit and Mandal, 2020).

Seismic Attributes

To detect strong or weak amplitudes (bright spots or dim spots) and to create invisible features in the seismic data within specific intervals or zones visible, the seismic attribute analysis was utilized in this work. Since it accurately depicts the acoustic impedance contrast of a reflector, the seismic characteristic is a useful tool for highlighting strong reflectivity anomalies. Each attribute was used in a distinctive manner to support distinct purposes of explanation. These characteristics may consist of energy (instantaneous amplitude), low frequencies and sweetness (instantaneous amplitude divided by the square-root of instantaneous frequency), which are signs that there are hydrocarbons inside a trap (Bueno *et al*., 2014; Ferreira *et al*., 2021; Liu *et al*., 2022). In this study, seismic attributes (instantaneous amplitude, frequency, and sweetness) were used to assist the seismic DHI analysis between the clay of Klasafet Formation and the reef limestone of Kais Formation.

Seismic Spectral Decomposition

Spectral decomposition is employed to display temporal layer thicknesses in order to satisfy reservoir delineations, including the detection and differentiation of limestone reef, shale resources, stratigraphic assessments, and indications of fluid content (*i.e.* hydrocarbon oil or gas) (Partyka *et*

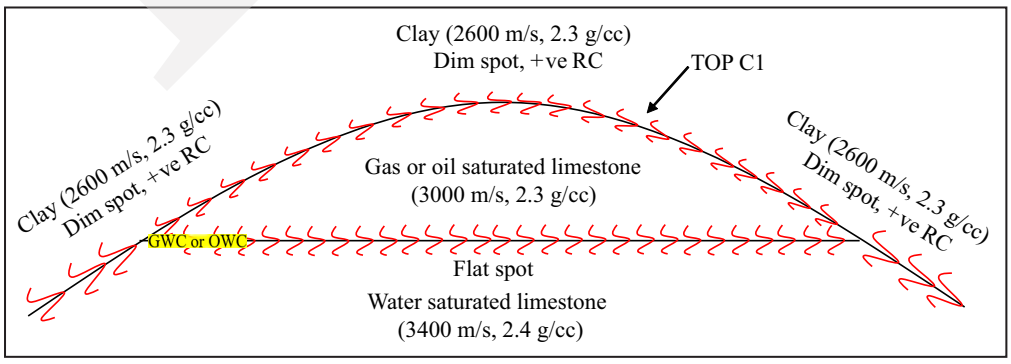

Figure 3. Scheme of the seismic direct hydrocarbon indicator (DHI) of the studied area (modified from Nanda *et al*., 2021).

al., 1999; Marfurt and Kirlin, 2001; Castagna *et al*., 2003). One of the spectral decomposition technologies, Continuous Wavelet Transform (CWT), allows seismic signals to be examined in the time and frequency domain simultaneously. It has an ideal time-frequency resolution property, and has turned out to be a well-known tool for the investigation of seismic data (Sinha *et al*., 2005; Xue *et al*., 2014; Naseer, 2018; 2023). In this study, CWT was applied in different frequency windows 10 Hz, 20 Hz, and 30 Hz to characterize fluid response in carbonate reservoir rocks of Kais Formation.

Materials

The seismic data was acquired by TGS Nopec company in Salawati Basin, West Papua (Figure 4). The seismic recording scheme was a 636-streamer group system. The seismic source was a 2000 Psi Soldera G-Gun. The acquisition geometry was designed with a 25 m shot spacing and a 12.5 m receiver interval. The sample rate was 2 ms and the total recording time was 9,000 ms (Table 1). The total lenght of the seismic line is 7,950 m acquired in 2010.

The South Salawati survey was completed with a significant emphasis on turnover and in accordance with the frontier basin processing flow established in 2008. Multiple energy was present, and the use of multiple removal techniques was tested outside of the confirmation flow as needed. This multiple energy was greatly reduced by using SRME and Tau-P deconvolution in the shot domain, as well as Radon demultiple (two rounds) and Residual Radon demultiple in the CDP domain. However, it still exists to variable degrees in regions where the seabed is undulated or rough, or when multiple energies are created from beyond the plane.

Table 1. Seismic Parameter of the Salawati Field

DESCRIPTION	DETAILS
Seismic source	Soldera G-Gun
Pressure	2000psi
Depth	5 m
Source interval	25 m
Record length	9000 ms
Sample interval	2 ms
Streamer length	7950 m
Streamer depth	7 m
Group interval	12.5 m

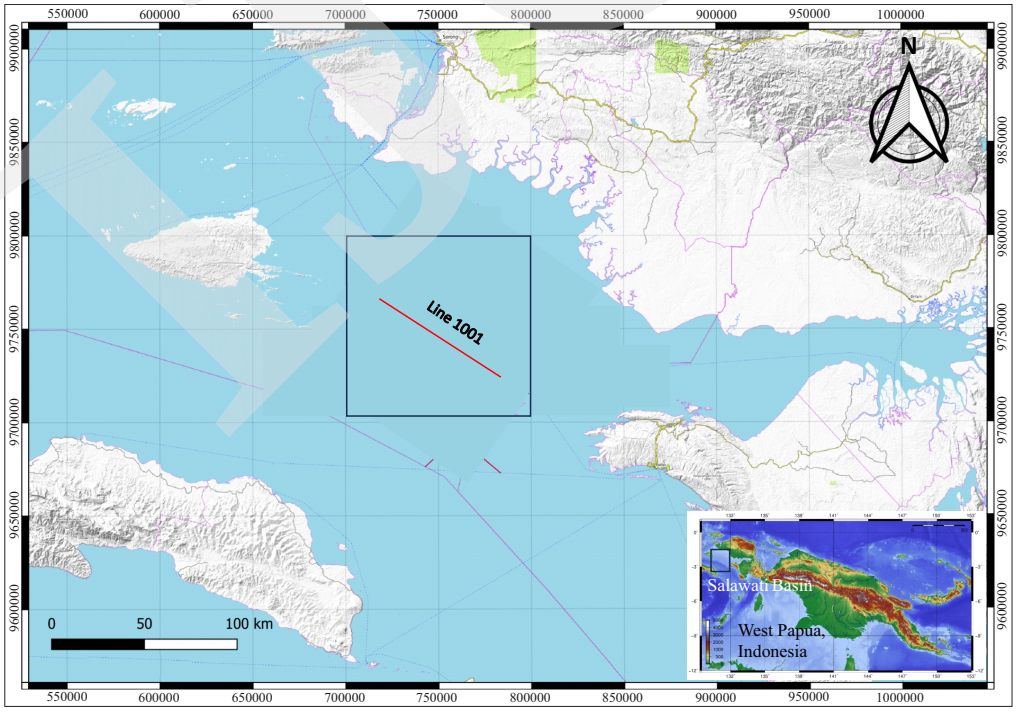

Figure 4. Location of the Salawati Field and the seismic line 1001 (red line).

The presence of swell, linear, and random noise was reduced as much as possible in the shot domain using time frequency denoise and three rounds of TauP linear noise attenuation. Prior to PSTM, Ranna and FK filters were employed in the common offset domain to suppress linear and random noise. TGS experts the three passes of closely spaced velocity studies (1 km, 1 km, and 0.5 km intervals), and every line was restacked at each level of QC to ensure that any changes made improved the data coherency. Constant velocity analyses were created to help identify the right velocity trends in areas of complex geology and where there were uncertainties about velocity trends.

Result and Analysis

2D Seismic Result

The seismic section along NW to SE are shown in Figure 5a, and the seismic frequency spectra are shown in Figure 5b. Based on seismic response in Figure 5a, the interest zone is identified as a reef carbonate geometry associated with the reef limestone of the Kais Formation with the upper part of the limestone symbolized by C1 (black rectangle). In Figure 5b, the frequency content in this region is mostly distributed between 10 - 50 Hz frequency band.

Seismic records of the Kais Formation generally have the appearance of parallel to subparallel reflections. This reflection shows that the Kais Formation was generally deposited in a stable environment. Lagoon is characterized by the appearance of parallel reflections and medium to high amplitude, pinnacle reef is characterized by the appearance of strong reflections with weak internals like a patch reef, but has a pointed shape at the top C1 (Figure 5a). The lower boundary of the Kais Formation is not drawn with a clear line, because its appearance only displays chaotic reflections, so that only colour gradations are given which indicate that at the lower boundary of the Kais Formation there are thought to be other formations, but the boundaries are not visible.

Seismic Interpretation and DHI

In Figure 6b, the top C1 is identified as a positive reflectivity contrast, going from shaly Klasafet Formation to limestone reef of Kais Formation. Direct indicators of hydrocarbons are seen at various depth levels in the reef limestone

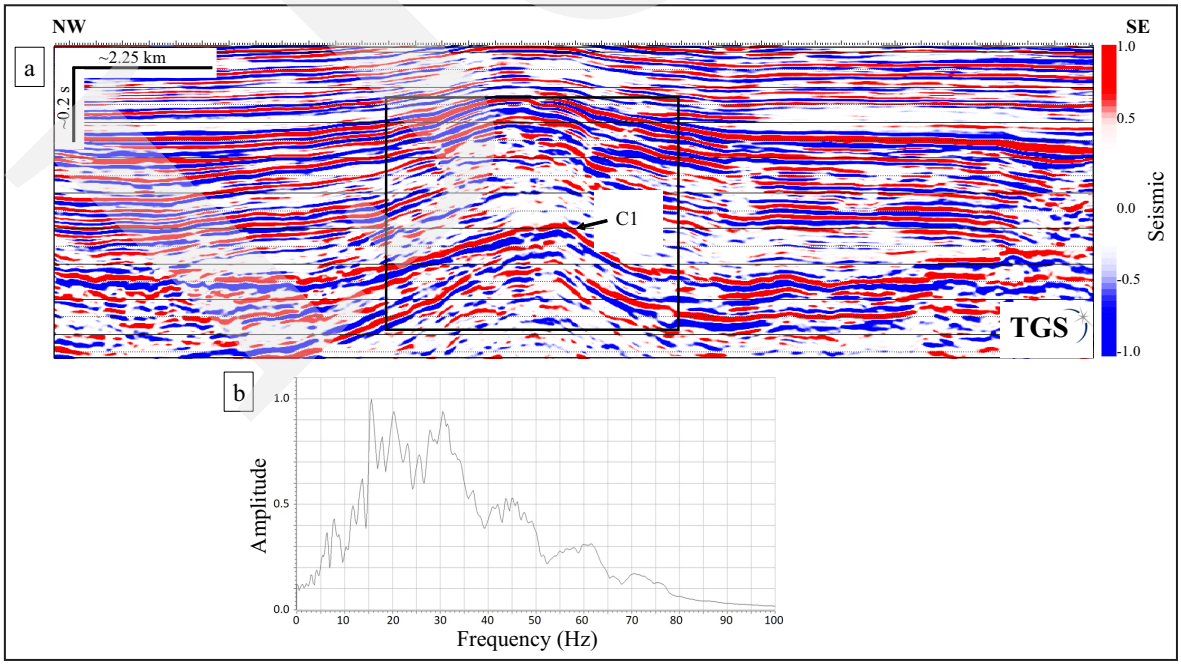

Figure 5. Displays of seismic profile of the studied area. (a) Seismic section with the highlighted zone of interest and (b) Amplitude versus frequency spectrum of the interest zone.

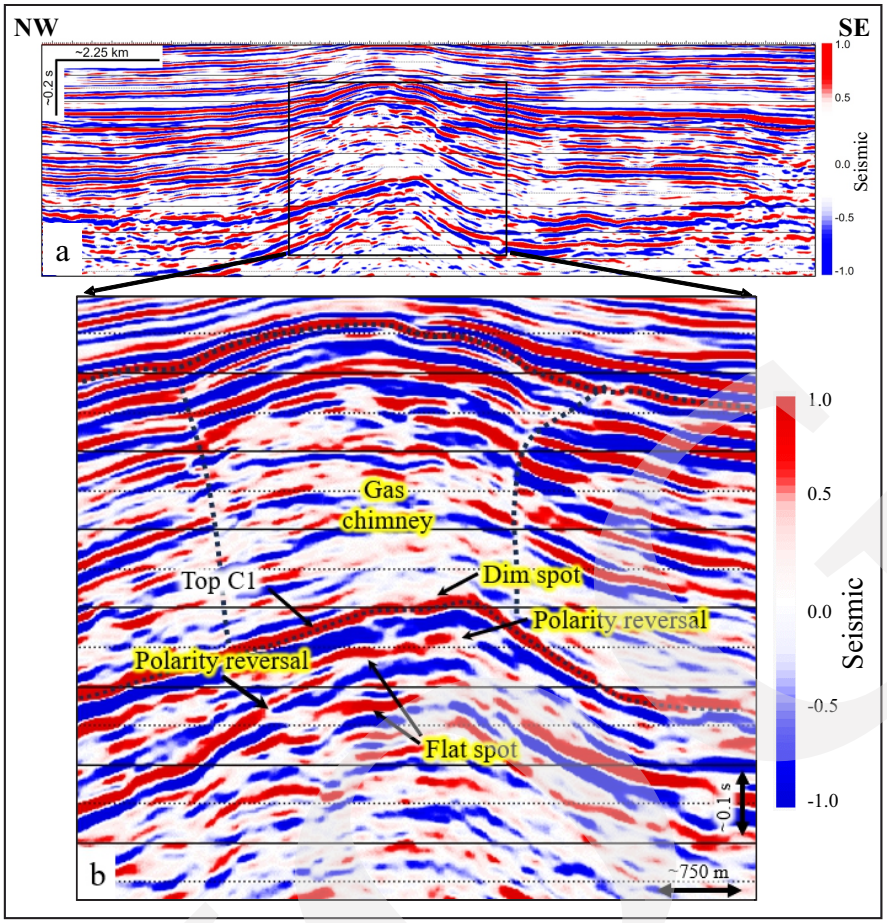

Figure 6. Interpretation of DHI of reef limestone of Kais Formation: (a) Original section and (b) Detailed of reef limestone of Kais Formation with DHI: gas chimney, dim spot, flat spot, and polarity reversal.

from Early Miocene to Late Miocene of Kais Formation. These indicators consist of gas chimneys, dim spots, flat spots, polarity reversal, and low frequency. A gas leak (gas chimney) on a seismic profile is regarded as a seismic exception, meaning that it resulted in wave field scattering and absorption rather than reflection (Petersen *et al*., 2010; Dixit and Mandal, 2020). Both the partial gas saturation inside the gas chimney and the heterolithic nature of the shaly Klasafet Formation are causing frequency dependent wavefield attenuation (*i.e.* absorption and scattering attenuation, respectively), which results in a poor seismic reflection quality.

The seismic section existing in the Kais Formation allows for the obvious recognition of the DHIs criteria (dim spots, flat spots, and polarity reversals) as well as some of the characteristics of reef limestone (Figure 6b). Dim spots were identified on the boundary between the Klasafet Formation and the Kais Formation on the top reef limestone C1 which was caused by a change in the low acoustic impedance of the Klasafet Formation clay to the high acoustic impedance of the Kais Formation limestone. The presence of gas in the limestone will cause a relative dimming of the seismic reflectivity, relative to brine-filled limestone. Then, numerous flat spots manifested as horizontal red reflectors are observed within the limestone reef of Kais Formation. These are linked to slight changes in acoustic impedance between the water saturated limestone beneath oil or gas saturated limestone filling the upper part of the carbonate reservoir (Chopra and Marfurt, 2012; Kluesner *et al*., 2013; Neidell and Charuk, 2018). Finally, another indication that the presence of hydrocarbons in the reservoir causes the velocity to drop is the DHI seismic polarity

reversal that occurred in the limestone of the Kais Formation. This reversal of polarity in the zone of interest may be due to sudden differences in the physical characteristics of nearby lithofacies or due to the presence of hydrocarbons (Barnes, 2001; Nanda, 2021).

Seismic Attributes

The instantaneous amplitude contour X-section is displayed in Figure 7b. On the map, there are distinct zones of moderate to high amplitude (1,000 – 1,200 positive amplitude). These moderate to high amplitude values are frequently linked to lithological changes such as a high porosity (porous limestone) (Bueno *et al*., 2014; Xue *et al*., 2018 Ferreira *et al*., 2021; Liu *et al*., 2022), dark areas, and particularly reef limestone zones of Kais Formation that were saturated with gas or oil. Then, by taking the instantaneous phase as a function of time derivative, the average instantaneous frequency attribute is calculated. In Figure 7c, low frequency zones (10 - 30 Hz) are present in more than half the portion of the cross section. Low frequencies are frequently linked to fracturing, lithology changes, hydrocarbon-saturated reservoirs, and especially gas-saturated reservoirs (*i.e.* reef limestone of Kais Formation) (Castagna *et al*., 2003; Zeng, 2010; Xue *et al*., 2018). Finally, in Figure 7d, the high value sweetness attribute (the ratio between high instantaneous amplitude and low frequency) around 1,500 - 2,250 envelope is observed on top C1 correlated to the top of reef limestone of Kais Formation. The high sweetness characteristic typically correlates with the reservoir rock hydrocarbon (oil or gas) content (Hart *et al*., 2002; Sena *et al*., 2011; Wang *et al*., 2016).

Seismic Spectral Decomposition

In Figure 8, there are three different spectral frequencies from CWT method. In Figure 8b, in low frequency of 10 Hz, high amplitude was detected on the top of C1. The low frequency that is observed on top C1 may be correlated to hydrocarbon response on the limestone reef of Kais Formation (Smith, 2009; Yang *et al*., 2014; Farfour *et al*., 2015). Then the amplitude was decreased in frequency 20 Hz (Figure 8c) and 30 Hz (Figure 8d) which was caused by attenuation

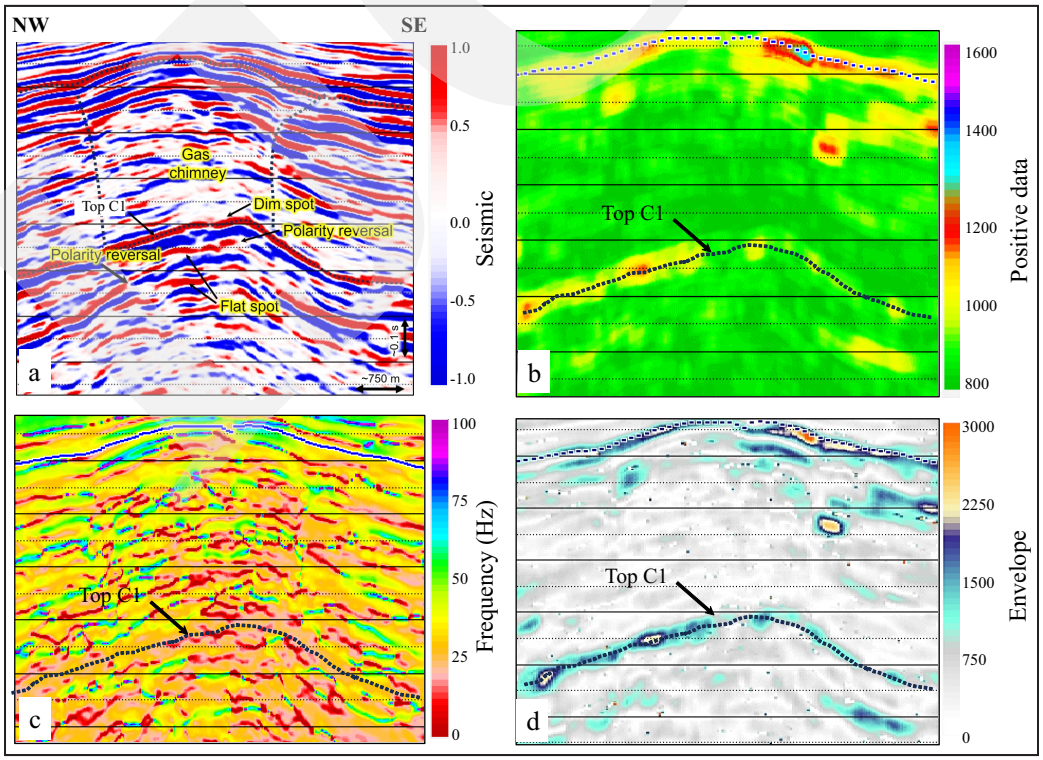

Figure 7. Seismic attributes on studied area: (a) Original section; (b) Instantaneous amplitude; (c) Instantaneous frequency; and (d) Sweetness attribute.

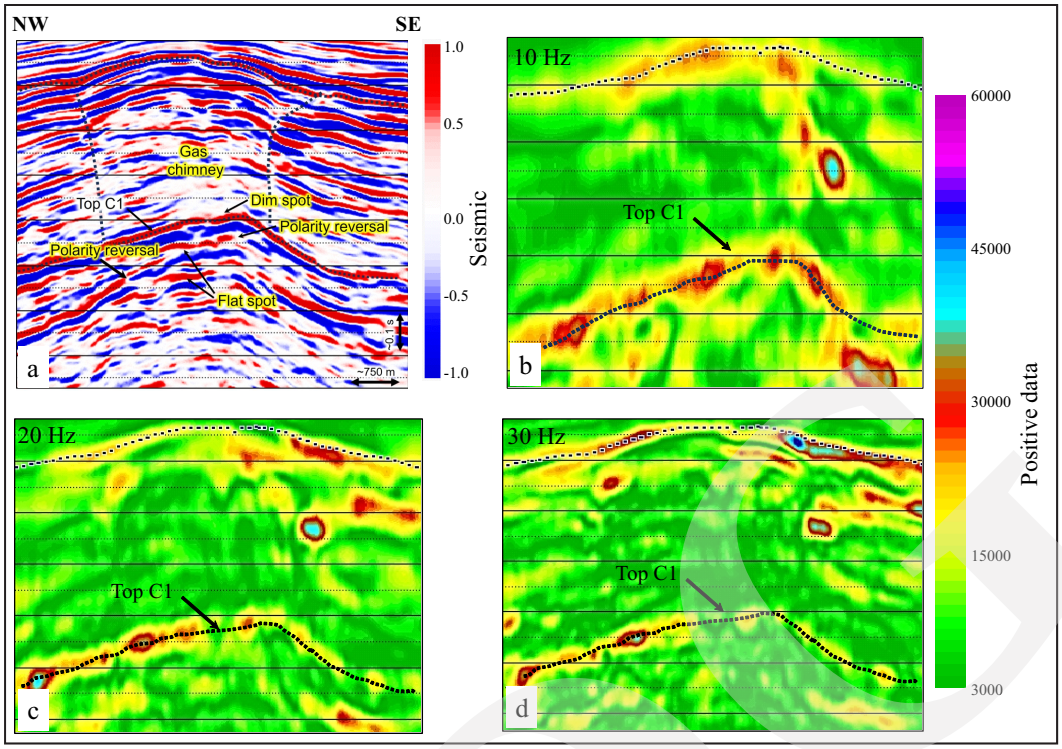

Figure 8. Seismic CWT maps of the studied area: (a) Original section; (b) Spectral frequency 10 Hz; (c) Spectral frequency 20 Hz; and (d) Spectral frequency 30 Hz.

mainly due to the presence of fluid in the reservoir rock (Mavko and Dvorkin, 2005; Quintal *et al*., 2009; Chen, 2020). In addition, the most beneficial outcomes for identifying hydrocarbons come from the spectrum decomposition of the CWT method at frequencies between 10 Hz and 20 Hz since this range of frequencies is tuned to represent the lateral distribution of hydrocarbons with low frequency values.

Dicussion

Seismic Response of Fluid Content

The existence of hydrocarbon fluids in reservoir rocks using the available geological and geophysical data is one of the key stages in hydrocarbon exploration. Fluid saturation within rock strata can initially be detected through amplitude and frequency responses in relatively new fields when only geophysical data is available (for example seismic sections). Dim spots, bright spots, and flat spots are examples of DHI information that can be obtained from amplitude fluctuations in magnitude. Meanwhile, the DHI polarity reversal indicator can be used to identify the hydrocarbon potential zone based on the change in phase/polarity (Chopra and Marfurt, 2012; Kluesner *et al*., 2013; Neidell and Charuk, 2018).

In this study, dim spots, flat spots, and polarity reversal—all DHI indicators—were observed on the reef limestone of the Kais Formation (Figure 6b). These zones may have hydrocarbon oil or gas potential, as evidenced by dim spots at the boundary between the shaly Klasafet Formation and the top reef limestone of the Kais Formation. Based on an earlier research, dim spots in carbonate rocks are a sign that the lithology is shifting from the shale/clay horizon to the top carbonate reservoir, and that the presence of hydrocarbon fluids leads to weaker contrasts in the elastic parameters compared to the same reservoir rocks filled with water (Forrest *et al*., 2010; Zdanowski and Górniak, 2014; Howarth and Alves, 2016). Further investigations of the internal seismic reflectors in the Kais Formation limestone, reveals multiple horizontal events or flat spots (Figure 9a), interpreted as pore fluid contacts between hydrocarbons and water (Chopra and Marfurt, 2012; Kluesner *et al*., 2013; Neidell

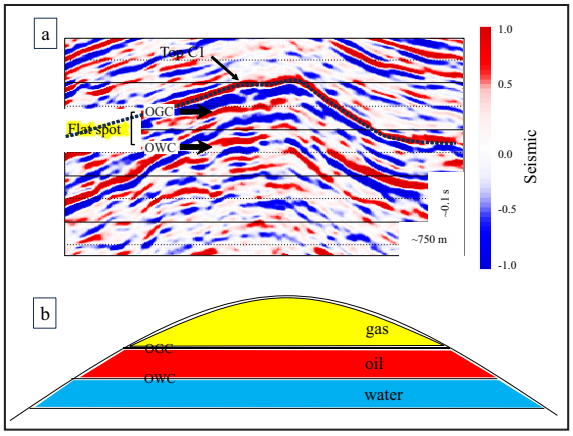

Figure 9. Interpretation of multiple flat spots in this study. (a) Interpretation of oil-gas contact (OGC) and oil-water contact (OWC) from seismic DHI. (b) Illustration of fluid content layers in the reservoir rock.

and Charuk, 2018). Figure 9a shows that, the two flat spots are regarded as a multiphase fluid composition that includes oil-gas contact (OGC) and oil-water contact (OWC) at a lower layer. Figure 9b indicates an illustration of the fluid arrangement in reservoir rocks where water is in the bottom layer because its density is the highest, gas is in the top layer because its density is the lightest, and oil is between the water and gas (Fustic *et al.*, 2019; Huang *et al.*, 2020; Jia *et al.*, 2023).

Then, polarity reversal was also observed on several horizons which seemed to be disconnected due to changes in reflector colour. Several previous studies have provided information that changes in polarity or seismic phase are inversely associated with the presence of fluid in rock layers due to a decrease in seismic velocity compared to its surroundings (Barnes, 2001; Nanda, 2021).

The results of seismic attribute data processing and spectral decomposition support the proof by demonstrating conformity with the DHI seismic results. The high acoustic impedance of the reef limestone of Kais Formation correlates with the high instantaneous amplitude attribute on the top C1 (Bueno *et al.*, 2014; Xue *et al.*, 2018; Ferreira *et a*l., 2021; Liu *et al.*, 2022). Therefore, the instantaneous frequency value confirms that the top C1 layer fluid content is the cause of the low anomaly in that layer, where several prior study findings have demonstrated that low frequencies are associated with the presence of fluid (Castagna *et al.*, 2003; Zeng, 2010; Xue *et al.*, 2018). Then, the target zone is further supported by the evidence that it contains hydrocarbon by dividing the amplitude value by frequency and obtaining a high sweetness attribute value on top C1 (Hart *et al.*, 2002; Sena *et al.*, 2011; Wang *et al.*, 2016). Additionally, the lateral frequency distribution is highly clearly mapped by the CWT result at a frequency of 10 - 20 Hz (Mavko and Dvorkin, 2005; Smith, 2009; Quintal *et al.*, 2009; Yang *et al.*, 2014; Farfour *et al.*, 2015; Chen, 2020).

Limitation of the Study

Even though the Salawati Basin prospect zones can be inferred from seismic DHI, seismic attributes, and spectral decomposition results, this research will be more reliable if well data is also incorporated. The key to this research will be the existence of well data, because drilling in the prospect zone is required to validate the prospect zone.

Furthermore, the seismic attribute procedure requires well data for error analysis and the iterative process of choosing the proper seismic attributes (Russell *et al.*, 1997; Zahmatkesh *et al.*, 2021; Haque *et al.*, 2022). Aside from spectral decomposition, the availability of well data would further increase the confidence of the prospect zone identification results, even if in some instances it can stand alone without well data as a preliminary study (Saeid *et al.*, 2020; Zhao and Zhang., 2021; Gu *et al.*, 2022). It is also envisaged that future studies would contain information on wells in the Salawati Basin region.

Proposed Well-test for the Next Exploration Steps

Based on seismic analysis in the researched area, the target zone is predicted to be very prospective as a hydrocarbon reservoir which is a carbonate reservoir (reef limestone, Kais Formation). Therefore, well data information at the researched location is needed. The recommended location for the well test is placed in an area that can penetrate the reef limestone layer of the Kais Formation (Figure 10). The goal to be

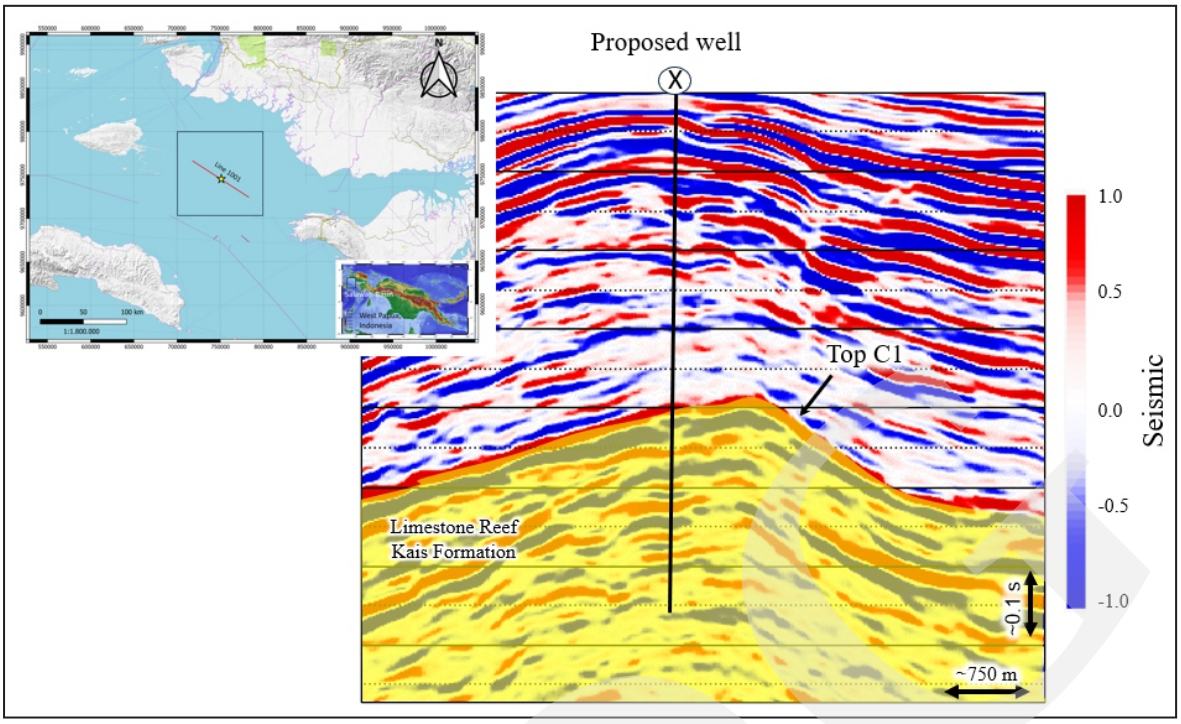

Figure 10. Location of the proposed well-test in the reef limestone of Kais Formation, Salawati Basin, West Papua.

achieved is that the drill hole can penetrate layers that are likely to contain hydrocarbons in the interest zone. Previous research has also showed that hydrocarbon prospect zones in carbonate rocks are located at the top of carbonate growth, although this is analogous to high areas in clastic reservoirs (Baldini *et al*., 2020; Hu *et al*., 2020; Radwan *et al*., 2022; Sun *et al*., 2023).

Conclusions

This research is an initial study of a new prospect zone around the Salawati Basin, West Papua, eastern Indonesia. Analysis of carbonate geometry and fluid content within it can be an initial screening stage in the hydrocarbon exploration process. From the seismic characterization of the studied area, it was obtained that the reservoir geometry of the target zone correlated with the reef limestone of Kais Formation. Then, in an internal analysis of the reservoir geometry regarding seismic amplitude and frequency values, information was obtained that the target zone was a reservoir layer containing hydrocarbons as observed by seismic DHI flat spots, dim spots, and polarity reversal. Seismic attribute instantaneous amplitude, frequency, and sweetness data also confirm that the target zone contains the presence of hydrocarbon fluids. In addition, CWT analysis provides information on the lateral distribution of low frequencies 10 - 20 Hz following the top C1 reef limestone of Kais Formation.

This study suggests doing tests utilizing well data that is right above the reef limestone of The Kais Formation on the surface. This well test is recommended to be carried out at the advanced exploration stage. It is expected that this well will reach the target zone and provide evidence that in fact it is proven to be an effective reservoir rock.

Acknowledgments

The authors thank TGS Nopec Company for the permission to use the seismic data in this research and Institut Teknologi Sumatra (ITERA), DIG Science.

References

Arntsen, B., Wensaas, L., Løseth, H., and Hermanrud, C., 2007. Seismic modeling of gas chimneys. *Geophysics*, 72 (5), SM251 - 259. DOI: 10.1190/1.2749570

Avseth, P. and Lehocki, I., 2021. 3D subsurface modeling of multiscenario rock property and AVO feasibility cubes-An integrated workflow. *Frontiers in Earth Science,* 9, *642363.*

Baldini, D., Piazza, L., and Barbanotti, L., 2020, January. Artificial intelligence and machine learning techniques provide operations geologists with an automated and reliable lithology-fluid pattern recognition assistant: A case history in a clastic reservoir in West Africa. *International Petroleum Technology Conference,* p.D021S031R001). IPTC. DOI: 10.2523/iptc-19701-ms

Barnes, A.E., 2001. Seismic attributes in your facies. *CSEG recorder,* 26 (7), p.41-47.

Bueno, J.F., Honório, B.C.Z., Kuroda, M.C., Vidal, A.C., and Leite, E.P., 2014. Structural and stratigraphic feature delineation and facies distribution using seismic attributes and well log analysis applied to a Brazilian carbonate field. *Interpretation,* 2 (1), *SA83-92*. DOI: 10.1190/int-2013-0087.1

Castagna, J.P., Han, D.H., and Batzle, M.L., 1995. Issues in rock physics and implications for DHI interpretation. *The Leading Edge*, 14 (8), p.883-886.

Castagna, J.P., Sun, S., and Siegfried, R.W., 2003. Instantaneous spectral analysis: Detection of low-frequency shadows associated with hydrocarbons. *The leading edge,* 22 (2), p.120-127. DOI: 10.1190/1.1559038

Chen, H., 2020. Seismic frequency component inversion for elastic parameters and maximum inverse quality factor driven by attenuating rock physics models. *Surveys in Geophysics,* 41 (4), p.835-857.

Chopra, S. and Marfurt, K.J., 2012. Seismic attribute expression of differential compaction. *The Leading Edge,* 31 (12), p.1418-1422. DOI: 10.1190/tle31121418.1

Cooke, D.A., 1993. Reservoir interval velocities derived from seismic pull-up: A Java Sea case history of a new seismic DHI. *SEG Technical Program Expanded Abstracts*, p.823-824. Society of Exploration Geophysicists. DOI: 10.1190/1.1822628

Dixit, A. and Mandal, A., 2020. Detection of gas chimney and its linkage with deep-seated reservoir in Poseidon, NW shelf, Australia from 3D seismic data using multi-attribute analysis and artificial neural network approach. *Journal of Natural Gas Science and Engineering,* 83, 103586.

Do Nascimento, L.F., Vincentelli, M.G.C., and de Jesus Perinotto, J.A., 2017. GEOLOGICAL SETTINGS AND SEISMIC ATTRIBUTES IN ALBIAN CARBONATES RESERVOIRS-SOUTHWEST OF CAMPOS BASIN (RJ-BRAZIL). *Brazilian Journal of Geophysics,* 35 (2), p. 109-121. DOI: 10.22564/rbgf.v35i2.808

Dow, D.B. and Sukamto, R., 1984. Western Irian Jaya: the end-product of oblique plate convergence in the Late Tertiary. *Tectonophysics,* 106 (1 - 2), p.109-139.

Farfour, M., Yoon, W.J., and Kim, J., 2015. Seismic attributes and acoustic impedance inversion in interpretation of complex hydrocarbon reservoirs. *Journal of Applied Geophysics,* 114, p.68-80. DOI: 10.1016/j.jappgeo.2015.01.008

Ferreira, D.J.A., Dias, R.M., and Lupinacci, W.M., 2021. Seismic pattern classification integrated with permeability-porosity evaluation for reservoir characterization of presalt carbonates in the Buzios Field, Brazil. *Journal of Petroleum Science and Engineering,* 201, 108441.

Forrest, M., Roden, R., and Holeywell, R., 2010. Risking seismic amplitude anomaly prospects based on database trends. *The Leading Edge,* 29 (5), p.570-574. DOI: 10.1190/1.3422455

Fustic, M., Strobl, R., Fowler, M., Jablonski, B.V., and Martinius, A.W., 2019. Impact of reservoir heterogeneity on oil migration and the origin

of oil-water contacts: McMurray Formation type section, Alberta, Canada. *Marine and Petroleum Geology,* 103, p.216-230.

Gu, J., Peng, Y., Lu, H., Chang, X., and Chen, G., 2022. A novel fault diagnosis method of rotating machinery via VMD, CWT and improved CNN. *Measurement,* 200, 111635. DOI: 10.1016/j.measurement.2022.111635

Hamilton, W., 1979. Tectonic of the Indonesia Region. *U.S. Geological Professional Paper,* 1078, 345pp.

Handoyo, H., Erlangga, M.P., and Young, P., 2020. Rock Physics Formula and RMS Stacking Velocity Calculation to Assist Acoustic Impedance Inversion that Constrain Well Data. *Journal of Geoscience, Engineering, Environment, and Technology,* 5 (2), p.56-58. DOI: 10.25299/jgeet.2020.5.2.3089

Haque, A.E., Qadri, S.T., Bhuiyan, M.A.H., Navid, M., Nabawy, B.S., Hakimi, M.H., and Abd-El-Aal, A.K., 2022. Integrated wireline log and seismic attribute analysis for the reservoir evaluation: A case study of The Mount Messenger Formation in Kaimiro Field, Taranaki Basin, New Zealand. *Journal of Natural Gas Science and Engineering,* 99, 104452. DOI: 10.1016/j.jngse.2022.104452

Hart, B.S., Pearson, R., and Rawling, G.C., 2002. 3-D seismic horizon-based approaches to fracture-swarm sweet spot definition in tight-gas reservoirs. *The Leading Edge,* 21(1), p.28-35.

Howarth, V. and Alves, T.M., 2016. Fluid flow through carbonate platforms as evidence for deep-seated reservoirs in northwest Australia. *Marine Geology,* 380, p.17-43. DOI: 10.1016/j.margeo.2016.06.011

Hu, Y., Peng, X., Li, Q., Li, L., and Hu, D., 2020. Progress and development direction of technologies for deep marine carbonate gas reservoirs in The Sichuan Basin. *Natural Gas Industry B,* 7 (2), 149-159.

Huang, J., Jin, T., Chai, Z., Barrufet, M., and Killough, J., 2020. Compositional simulation of three-phase flow in mixed-wet shale oil reservoir. *Fuel,* 260, 116361. DOI: 10.1016/j.fuel.2019.116361

Jia, L., Zhong, L., Ge, H., and Shen, Y., 2023. Effect of crude oil self-emulsification on the recovery of low permeability reservoir after well soaking. *Journal of Petroleum Science and Engineering,* 2 (20), 111201.

Kluesner, J.W., Silver, E.A., Bangs, N.L., McIntosh, K.D., Gibson, J.C., Orange, D., Ranero, C.R., and von Huene, R., 2013. High density of structurally controlled, shallow to deep water fluid seep indicators imaged offshore Costa Rica. *Geochemistry, Geophysics, Geosystems*, 14 (3), p.519-539. DOI: 10.1002/ggge.20058.

Li, Q., Di, B., Wei, J., Yuan, S., and Si, W., 2016. The identification of multi-cave combinations in carbonate reservoirs based on sparsity constraint inverse spectral decomposition. *Journal of Geophysics and Engineering,* 13 (6), p.940-952. DOI: 10.1088/1742-2132/13/6/940

Li, Y., Zheng, X., and Zhang, Y., 2011. High-frequency anomalies in carbonate reservoir characterization using spectral decomposition. *Geophysics,* 76 (3), V47-57.

Liu, Y. and Wang, Y., 2017. Seismic characterization of a carbonate reservoir in Tarim Basin. *Geophysics,* 82 (5), B177-188. DOI: 10.1190/geo2016-0517.1

Liu, R., Guo, R., Liu, N., Zhu, G., Liu, X., Ning, C., and Hua, G., 2022. Multifrequency Analysis via LTSA and Its Application on Carbonate Reservoir Delineation. *IEEE Geoscience and Remote Sensing Letters,* 19, p.1-5. DOI: 10.1109/lgrs.2022.3227170

Marfurt, K.J. and Kirlin, R.L., 2001. Narrow-band spectral analysis and thin-bed tuning. *Geophysics,* 66 (4), p.1274-1283.

Mavko, G. and Dvorkin, J., 2005. P-wave attenuation in reservoir and non-reservoir rock. 67th European Association of Geoscientists and Engineers, EAGE Conference and Exhibition, incorporating SPE EUROPEC 2005-*Extended Abstracts*, p.1855-1858. Society of Petroleum Engineers. DOI: 10.3997/2214-4609-pdb.1.h033

Nanda, N.C., 2021. Direct hydrocarbon indicators (DHI). In Seismic Data Interpretation

and Evaluation for Hydrocarbon Exploration and Production. *A Practitioner's Guide*, p.117-129. Cham: Springer International Publishing.

Naseer, M.T. and Asim, S., 2018. Characterization of shallow-marine reservoirs of Lower Eocene carbonates, Pakistan: Continuous wavelet transforms-based spectral decomposition. *Journal of Natural Gas Science and Engineering,* 56, p.629-649. DOI: 10.1016/j.jngse.2018.06.010

Naseer, M.T. , 2023. Application of instantaneous spectral decomposition-based porosity simulations for imaging shallow-marine stratigraphic traps of Lower-Eocene carbonates sequences of Indus Basin, Onshore Pakistan. *Journal of Earth System Science,* 132 (1), 22.

Neidell, N.S. and Charuk, J., 2018. Seismic image undersampling—Resolution, visibility, and display. *The Leading Edge,* 37 (1), p.37-45. DOI: 10.1190/tle37010037 DOI: 10.1190/tle37010037.1

Palaz, I. and Marfurt, K.J., 1997. Carbonate seismology: An overview. Carbonate seismology: *Society of Exploration Geophysicists Geophysical Developments Series,* 6, p.1-7.

Partyka, G., Gridley, J., and Lopez, J., 1999. Interpretational applications of spectral decomposition in reservoir characterization. *The Leading Edge*, 18 (3), p.353-360. DOI: 10.1190/1.1438295

Petersen, C.J., Bünz, S., Hustoft, S., Mienert, J., and Klaeschen, D., 2010. High-resolution P-Cable 3D seismic imaging of gas chimney structures in gas hydrated sediments of an Arctic sediment drift. *Marine and Petroleum Geology,* 27 (9), p.1981-1994.

Phoa, R.S. and Samuel, L., 1986. Problems of source rock identification in The Salawati Basin, Irian Jaya. DOI: 10.29118/ipa.416.405.421

Pireno, G.E., 2017. Potensi Formasi Sirga Sebagai Batuan Induk di Cekungan Salawati, Papua. (Tesis Magister, Institut Teknologi Bandung), https://digilib.itb.ac.id/gdl/view/15745/cekungansalawati? rows=831&per_page=4

Quintal, B., Schmalholz, S.M., and Podladchikov, Y.Y., 2009. Low-frequency reflections from a thin layer with high attenuation caused by interlayer flow. *Geophysics,* 74 (1), p.15-23. DOI: 10.1190/1.3026620

Radwan, A. E., Husinec, A., Benjumea, B., Kassem, A. A., Abd El Aal, A. K., Hakimi, M. H., 2022. Diagenetic overprint on porosity and permeability of a combined conventional-unconventional reservoir: insights from the Eocene pelagic limestones, Gulf of Suez, Egypt. *Marine Petroleum Geology*, 146, 105967. DOI:10.1016/j.marpetgeo.2022.105967

Redmond, J.L. and Koesoemadinata, R.P., 1976. Walio oil field and the Miocene carbonates of Salawati Basin, Irian Jaya, Indonesia.

Robinson, K.M., 1987. *An overview of source rocks and oils in Indonesia.*

Rosa, M.C. and Vincentelli, M.G.C., 2017. SEISMIC ATTRIBUTES ANALYSIS OF A PERMO-POROUS SYSTEM IN NEO-BARREMIAN-EOAPTIAN CARBONATES RESERVOIRS-CAMPOS BASIN (BRAZIL). *Brazilian Journal of Geophysics,* 35 (2), p.123-139. DOI: 10.22564/rbgf.v35i2.809

Russell, B., Hampson, D., Schuelke, J., and Quirein, J., 1997. Multiattribute seismic analysis. *The Leading Edge,* 16 (10), p.1439-1444.

Saeid, E., Kendall, C.S.C., Kellogg, J., and De Keyser, T., 2020. Sequence stratigraphic framework of Paleogene fluvial and marginal marine depositional systems of Llanos Foothills Colombia using log character & spectral decomposition. *Journal of South American Earth Sciences,* 97, 102419. DOI: 10.1016/j.jsames.2019.102419

Sapiie, B. and Cloos, M., 2004. Strike-slip Faulting in The Core of The Central Range of West New Guinea Ertsberg Mining District, Indonesia. *GSA Bulletin*, p. 277 - 293.

Satyana, A.H., 2003. Re-evaluation of the sedimentology and evolution of the Kais carbonate platform, Salawati Basin, eastern Indonesia: exploration significance. DOI: 10.29118/ipa.565.03.g.022

Sena, A., Castillo, G., Chesser, K., Voisey, S., Estrada, J., Carcuz, J., and Hodgkins, P., 2011. Seismic reservoir characterization in resource shale plays: Stress analysis and sweet spot discrimination. *The Leading Edge,* 30 (7), p.758-764.

Shadlow, J., 2014. A description of seismic amplitude techniques. *Exploration Geophysics,* 45 (3), p.154-163. DOI: 10.1071/eg13070

Sinha, S., Routh, P.S., Anno, P.D., Castagna, J.P., 2005. Spectral decomposition of seismic data with continuous-wavelet transform. *Geophysics,* 70 (6), p.19-25.

Smith, M., 2009. Bandwidth extension using harmonics. *11th International Congress of The Brazilian Geophysical Society & EXPOGEF 2009, Salvador, Bahia, Brazil, 24 - 28 August 2009,* p.1345-1348). Society of Exploration Geophysicists and Brazilian Geophysical Society. DOI: 10.1190/sbgf2009-288

Sudirja, H. and Robinson, G., 1986. Transgressive Development of Miocene Reefs, Salawati Basin, Irian Jaya. s.l., *Indonesian Petroleum Association 15th Annual Convention*. DOI: 10.29118/ipa.1286.377.403

Sun, H., Li, S., Liu, Z., Chang, B., Shen, C., and Cao, W., 2023. EOR technologies for fractured-vuggy carbonate condensate gas reservoirs. *Natural Gas Industry B,* 10 (4), p.352-360.

Teillet, T., Fournier, F., Zhao, L., Borgomano, J., and Hong, F., 2021. Geophysical pore type inversion in carbonate reservoir: Integration of cores, well logs, and seismic data (Yadana Field, offshore Myanmar). *Geophysics,* 86 (3), B149-B164. DOI: 10.1190/geo2020-0486.1

Vincentelli, M.G.C., Contreras, S.A.C., and Chaves, M.U., 2014. Geophysical Characterization of Albian Carbonates Reservoirs in Brazilian Basins: The Sweetness as a tool for carbonate reservoirs definition. *Brazilian Journal of Geophysics,* 32 (4), p.695-705.

Wang, Z., Gao, J., Lei, X., Cui, X., and Wang, D., 2016. Application of 3D seismic attributes to optimize the placement of horizontal wells within a tight gas sand reservoir, Ordos Basin, China. *Geophysics,* 81 (3), B77-B86. DOI: 10.1190/geo2015-0244.1

Xue, Y.J., Cao, J.X., Tian, R.F., Du, H.K., and Shu, Y.X., 2014. Application of the empirical mode decomposition and wavelet transform to seismic reflection frequency attenuation analysis. *Journal of Petroleum Science and Engineering,* 122, p.360-370.

Xue, Y.J., Du, H.K., Cao, J.X., Jin, D., Chen, W., and Zhou, J., 2018. Application of a variational mode decomposition-based instantaneous centroid estimation method to a carbonate reservoir in China. *IEEE Geoscience and Remote Sensing Letters,* 15 (3), p.364-368. DOI: 10.1109/lgrs.2017.2788467

Yang, Y.S., Li, Y.Y., and Cui, D.H., 2014. Identification of karst features with spectral analysis on the seismic reflection data. *Environmental earth sciences,* 71, p.753-761.

Yu, H., Zhang, Y., Li, J.S., and Xu, G.C., 2013. Identification of the carbonate reservoir based on spectral decomposition. *Progress in Geophysics,* 28 (3), p.1440-1446.

Zahmatkesh, I., Kadkhodaie, A., Soleimani, B., and Azarpour, M., 2021. Integration of well log-derived facies and 3D seismic attributes for seismic facies mapping: A case study from mansuri oil field, SW Iran. *Journal of Petroleum Science and Engineering,* 202, 108563. DOI: 10.1016/j.petrol.2021.108563

Zdanowski, P. and Górniak, M., 2014. Dim and bright spots as indicators of the Zechstein Main Dolomite hydrocarbon reservoir in Poland. *Interpretation,* 2 (4), SP17-30.

Zeng, H., 2010. Geologic significance of anomalous instantaneous frequency. *Geophysics,* 75 (3), p.23-30. DOI: 10.1190/1.3427638

Zhao, H. and Zhang, Y., 2021. *CWT-based method for extracting seismic velocity dispersion*. p.1-5.